IL NUOVO CIMENTO VOL. 36 B, N. 1 11 Novembre 1976

An Experimental Method for the Observation of R.F. Transitions and Laser Beat Resonances in Oriented Na Vapour.

G. ALZETTA, A. GOZZINI, L. MOI and G. ORRIOLS (*)

Laboratorio di Fisica Atomica e Molecolare del C.N.R. - Pisa

(ricevuto il 18 Agosto 1976)

Summary. — A method which allows a direct picture of phenomena involving line broadening, light shifts and many-photon transitions in the ground state of sodium atoms pumped by dye-laser is reported. A new phenomenon due to light beats between the different dye-laser axial modes has been easily evidenced by the method.

1. – Introduction.

A technique is reported which, by a simple modification of the usual equipments, results to be particularly convenient for the observation of magnetic transitions and related phenomena in alkali vapours oriented by dye-lasers. As is well known [1], in optical-pumping experiments Helmholtz coils are used in order to provide a well-defined quantization axis z in the direction of the pumping light and a uniform magnetic field all over the volume of the cell. Usually, the occurrence of a magnetic resonance is detected either by

(*) On leave of absence from the Departament d'Optica, Universidad de Barcelona, Barcelona, España.

(1) For a review of optical pumping: J. BROSSEL: in *Quantum Optics and Electronics*, edited by C. DE WITT and A. BLANDIN (New York, N. Y., 1965); C. COHEN-TANNOUDJI and A. KASTLER: in *Progress in Optics*, Vol. 5, edited by E. WOLF (Amsterdam, 1966); W. HAPPER: *Rev. Mod. Phys.*, **44**, 169 (1972); L. C. BALLING: in *Advances in Quantum Electronics*, Vol. 3, edited by D. W. GOODWIN (London, 1975).

the change of the transparency of the vapour in a longitudinal observation, or by the increase of the fluorescence in a transversal observation.

Now it is worthwhile to remark that the performance of the optical pumping is by no means affected if the magnetic field has a gradient along z, owing to the fact that the direction, and not the value of the magnetic field, provides the quantization axis. In this case, while optical pumping will lead to such an orientation of the vapour as the one of the uniform magnetic field, the Zeeman splitting of the ground-state sublevels results to be a function of z (see fig. 1). The resonances will occur only in the regions of the cell where the magnetic field and the frequency of the r.f. field fulfil the resonance condition

$$h\nu = g\beta H_z^0, \tag{1}$$

where g is the Landé factor and β is the Bohr magneton. Therefore, the decrease of transparency and the induced fluorescence of the vapour appear only in correspondence of the surface on which the magnetic field has the resonance value.

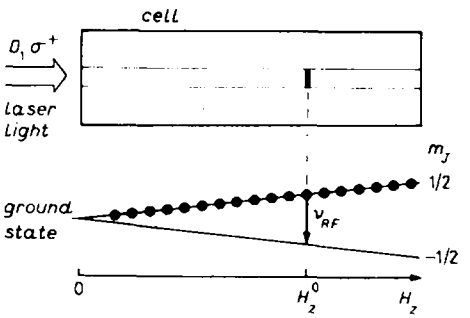

Fig. 1. – A diagram illustrating the principle of the method for a system with $J = \frac{1}{2}$ and $I = 0$.

By using a laser as source for the optical pumping, the pumped region can be reduced to a cylinder with the diameter of the light beam. In this case the surfaces $H_z = \text{const}$ are planes orthogonal to the beam axis. In a transversal observation the resonances will, therefore, appear as bright lines or spots due to the fluorescence induced by the r.f. transitions.

2. – Apparatus and experimental procedure.

Following the above-described principle, we adopted the experimental set-up shown in fig. 2. An Ar^+-laser pumps a c.w. dye-laser tuned on the

sodium D_1 line. The bandwidth of the axial modes of the dye-laser is about 0.3 Å at output power of the order of 0.5 W, and can be reduced to less than 0.1 Å with an etalon in cavity. The laser beam is circularly polarized by a quarter-wave plate and crosses a cell, heated up to 130 °C, containing saturated Na vapour and 40 Torr of neon as buffer gas. The cell is placed at the centre of a pair of Helmholtz coils. The gradient of the magnetic field along the beam is obtained by superposing to the uniform magnetic field the field given by an additional coil (gradient coil), coaxial with the Helmholtz coils. Two smaller coils can produce a r.f. field on the cell, perpendicular to the direction of the pumping-beam axis.

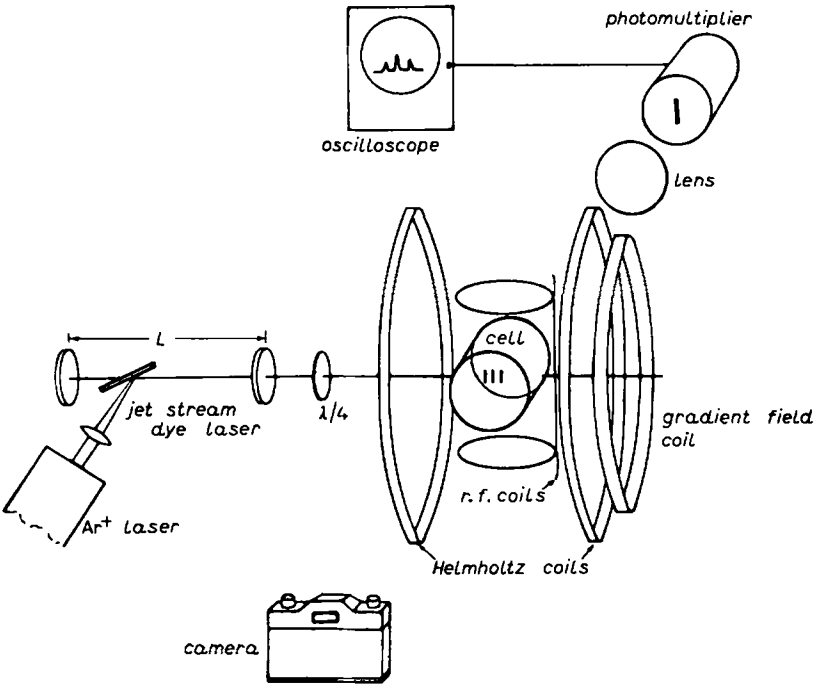

Fig. 2. – Experimental apparatus.

The resonances are observed laterally: the patterns can either be recorded on the film of a suitable camera or, by focussing it into a narrow slit in front of a photomultiplier, scanned as a function of the magnetic field.

The gradient field can be changed by varying the current of the supplementary coil, and the observed pattern can be expanded or narrowed as required for a suitable observation. The apparatus works therefore as a spectroscope with variable dispersion and resolution.

3. – Optical pumping by dye-laser and Zeeman magnetic resonances.

The output of our dye-laser consists of many axial modes with a mode spacing $\Delta\nu \simeq 290$ MHz, as outlined in fig. 3, where a comparison with the Doppler-broadened profile of the D_1 line is reported. The multimode pattern of the laser light forces us to consider the dependence of the excitation on the velocity distribution of the atoms ([2]). Owing to the Doppler effect, in a cell with uncoated walls and in the absence of any buffer gas, only a few per cent of the atoms can be pumped, the others being out of resonance. On the contrary, when buffer gas is introduced, the nondepolarizing collisions produce a pressure broadening of the atomic line and frequent velocity changes, so that the multimode laser can practically excite all the atoms to the $3P$ state.

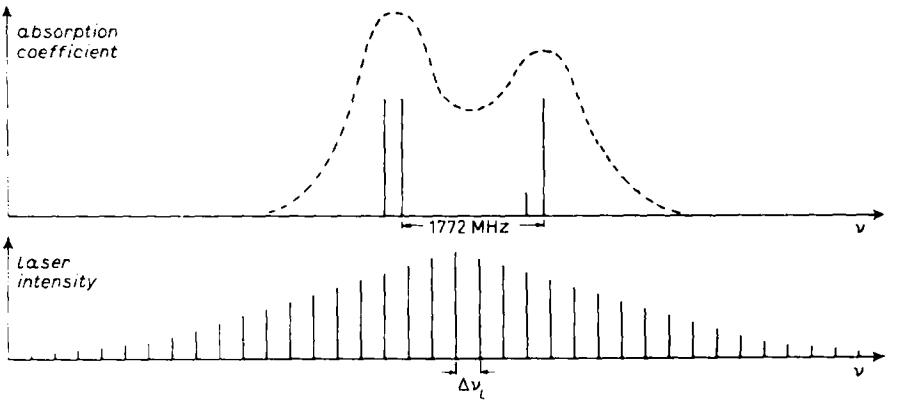

Fig. 3. – Spectral overlap between multimode laser radiation and D_1 absorption profile. (— — — Doppler profile of D_1 line).

In these conditions the optical-pumping cycle is equivalent to pumping with a « broad line » excitation. At high laser intensity, the thermal relaxation can be disregarded and a complete orientation of the vapour is realized. This can be monitored by the absence of fluorescence light along the pumping beam.

The $3\,^2S_{\frac{1}{2}}$ ground state of sodium ($I = \frac{3}{2}$) results, as indicated in fig. 10, in two hyperfine levels which, submitted to a weak magnetic field H_z, split in its Zeeman sublevels (F, m_F) unequally spaced owing to the Back-Goudsmit effect. The energy of the sublevels, $E(F, m_F)$, calculated with the Breit-Rabi formula ([3]) by neglecting the terms of order higher than the second in H_z

([2]) C. COHEN-TANNOUDJI: in *Atomic Physics*, Vol. **4** (New York, N. Y., and London, 1975), p. 589; M. DUCLOY: *Phys. Rev. A*, **8**, 1844 (1973); **9**, 1319 (1974).
([3]) F.i., see H. KOPFERMANN: *Nuclear Moments* (New York, N. Y., 1958).

(f.i., for $H_z \simeq 12$ G, the cubic terms are about 1 kHz), can be expressed as follows:

$$
(2) \qquad \left\{
\begin{aligned}
E(2,+2) &= \tfrac{3}{8}\Delta E_F + 2\gamma_2 H_z , \\
E(2,+1) &= \tfrac{3}{8}\Delta E_F + \gamma_2 H_z + 3\gamma' H_z^2 , \\
E(2,\ 0) &= \tfrac{3}{8}\Delta E_F + 4\gamma' H_z^2 , \\
E(2,-1) &= \tfrac{3}{8}\Delta E_F - \gamma_2 H_z + 3\gamma' H_z^2 , \\
E(2,-2) &= \tfrac{3}{8}\Delta E_F - 2\gamma_2 H_z , \\
E(1,-1) &= -\tfrac{5}{8}\Delta E_F + \gamma_1 H_z - 3\gamma' H_z^2 , \\
E(1,\ 0) &= -\tfrac{5}{8}\Delta E_F - 4\gamma' H_z^2 , \\
E(1,+1) &= -\tfrac{5}{8}\Delta E_F - \gamma_1 H_z - 3\gamma' H_z^2 ,
\end{aligned}
\right.
$$

where, if we measure E in MHz and H_z in G, $\Delta E_F = 1771.626$ MHz is the hyperfine splitting, and $\gamma_2 = 0.6998\,\mathrm{MHz \cdot G^{-1}}$, $\gamma_1 = 0.7021\,\mathrm{MHz \cdot G^{-1}}$, $\gamma' = 0.00028\,\mathrm{MHz \cdot G^{-2}}$ are related to the electronic Landé factor $g_J = 2.0023$ and to the nuclear factor $g_I' = 0.805 \cdot 10^{-3}$.

By pumping with σ^+ polarized intense laser light all the atoms are accumulated on the $(2, +2)$ sublevel. If the oriented vapour is submitted to a

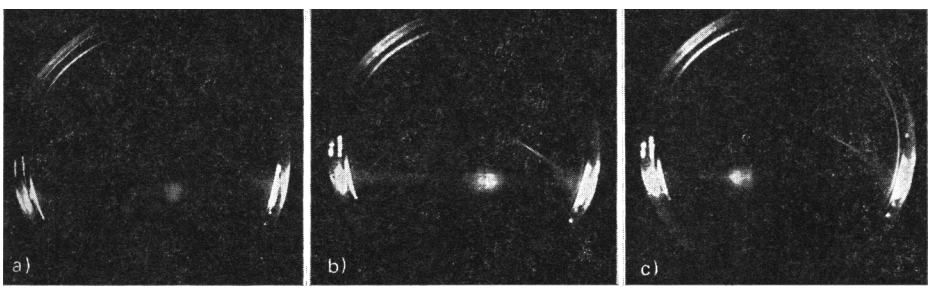

Fig. 4. – Fluorescence signals induced by a 5 MHz r.f. field: *a*) σ^+ pumping: $(2, +2;\ 2, +1)$ transition; *b*) r.f. power increased: $(2, +2;\ 2, +1)$ and $(2, +2;\ 2, 0)$ two-photon transitions; *c*) same power as in *b*), but with σ^- pumping radiation. The relative position of the $(2, -2;\ 2, -1)$ and $(2, -2;\ 2, 0)$ transitions is reversed and the pattern translated towards lower field.

weak radiofrequency field, the $(F, m_F;\ F', m_F') = (2, +2;\ 2, +1)$ transition is observed (fig. 4*a*)). By increasing the r.f. power, the $(2, +2;\ 2, 0)$, $(2, +2;\ 2, -1)$, $(2, +2;\ 2, -2)$ multiphoton transitions also appear at the different z values where the resonances occur. The lines show, besides a power broadening, radiative shifts due to the presence of other quasi-resonant

transitions with a common level [4] (f.i. the $(2, +2; 2, +1)$ will be shifted by the off-resonance $(2, +1; 2, 0)$ transition). In fig. 4*b*) the power-broadened $(2, +2; 2, +1)$ transition is visible, followed by the two-photon $(2, +2; 2, 0)$ transition. If the polarization of the pumping light is changed into σ^-, the $(2, -2)$ sublevel results to be populated and the $(2, -2; 2, -1)$ and $(2, -2; 2, 0)$ transitions are observed (fig. 4*c*)). Owing to the different separation of Zeeman sublevels, the lines appear in different places on the path of the beam and the relative position of the two-photon transition is reversed. The pictures of fig. 4 confirm that a practically complete pumping is obtained. In fig. 5 the positions of the one-, two- and three-photon lines are given as a function of the magnetic field for the two opposite polarizations.

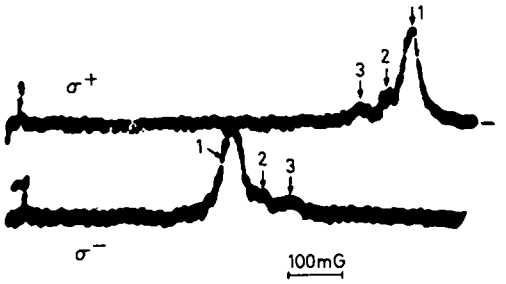

Fig. 5. – CRT traces showing the position of one-, two- and three-photon transitions for the two circular polarizations.

The CRT traces have been obtained by sweeping the field given by the Helmholtz coils and by recording the photomultiplier output as shown in fig. 2.

The effect of tuning the laser mode pattern on either sides of the D_1 line is shown in fig. 6. This effect manifests the « light shift » of the Zeeman

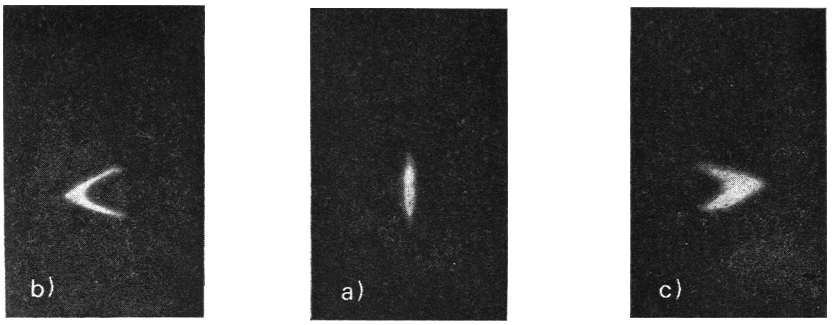

Fig. 6. – Light shift of $(2, +2; 2, +1)$ transition: *a*) laser tuned at the centre of the D_1 absorption line; *b*) laser tuned on the lower-frequency side of the D_1 line; *c*) laser tuned on the higher-frequency side of the D_1 line.

---

(4) J. M. WINTER: *Ann. de Phys.*, **4**, 745 (1959).

resonances ([5,6]) caused by nonresonant optical photons. In fig. 6*b*) and *c*) the laser mode pattern is tuned on both sides of the absorption line, and in fig. 6*a*) its centre coincides with the maximum of the D_1 absorption line. In this last case, « light broadening » of the r.f. resonances can be observed if the intensity of laser radiation is increased (fig. 7). The form of the lines points out the dependence of the shift and of the broadening on the intensity distribution across the laser beam, being the largest at the centre of the beam.

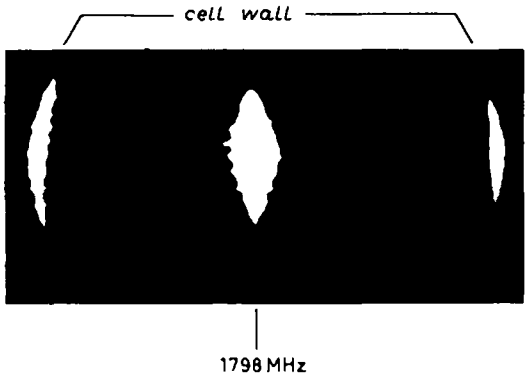

Fig. 7. – Broadening of the hyperfine (2, + 2; 1, + 1) transition due to the intense pumping light.

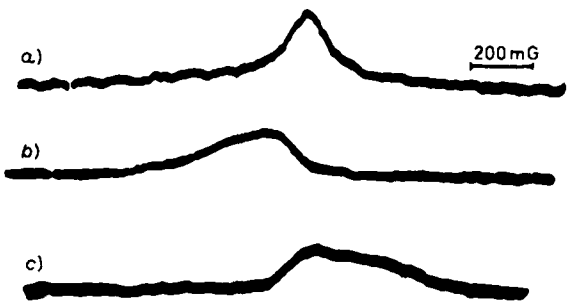

Fig. 8. – Oscilloscope traces showing the profile of the pattern of fig. 6 as obtained by photomultiplier observation.

The profiles of these lines, as observed on a CRT screen by scanning the pattern on the photomultiplier slit, are reported in fig. 8. We have measured shifts, at the centre of the beam, of the order of 500 kHz for a resonance at 8 MHz

---

([5]) J. P. BARRAT and C. COHEN-TANNOUDJI: *Journ. Phys. Rad.*, **22**, 328, 433 (1961).
([6]) C. COHEN-TANNOUDJI: *Ann. de Phys.*, **7**, 423, 469 (1962).

and pumping with 0.5 W of light power distributed in a beam of 0.1 cm^2 cross-section.

The light shift depends on the sign of the circular polarization, being of equal magnitude, but in opposite direction for opposite polarizations.

4. – Transitions involving hyperfine structure.

The method of the inhomogeneous magnetic field is very useful for more complex situations. An example is reported in fig. 9, where the pumped vapour is submitted simultaneously to two strong fields oscillating at hyperfine and Zeeman frequencies. The hyperfine field is produced by Lecker coils (omitted in fig. 2).

In fig. 9*a*) the fluorescence signal due to the (2, +2; 1, +1) hyperfine resonance is observed, at the z position where the static field has the value of 12.5 G. The transition is induced by a magnetic field H_1 ($\simeq 50$ mG), oscillating at the fixed frequency $\nu_1 = 1798$ MHz. Besides this field, the vapour is also submitted to a field H_2 ($\simeq 100$ mG), of a tunable lower frequency ν_2, which induces transitions between the Zeeman sublevels of the populated $F = 2$ hyperfine level. These do not appear in fig. 9*a*), where the H_z values for the Zeeman resonances fall outside the cell, owing to the chosen ν_2 frequency. If we reduce ν_2, the Zeeman resonances appear on the right-hand side of the hyperfine one (fig. 9*b*)). Owing to the r.f. power broadening, only the four-photon (2, +2; 2, −2) transition is clearly seen, the other transitions being mixed together in a broad single spot. Besides these multiphoton Zeeman resonances, another weak resonance is visible on the left of the hyperfine one. This is a two-photon hyperfine transition, connecting the (2, +2) and (1, 0) levels, via the intermediate (1, 1) level.

If the position of the Zeeman pattern is displaced near the right-hand side of the hyperfine resonance, another multiple quantum transition appears (fig. 9*c*)). This is a three-photon transition connecting the (2, +2) and (1, −1) levels, via the (1, +1) and (1, 0) intermediate levels. Finally, when the low-frequency resonances occur on the left side of the hyperfine one, a new line appears, that rapidly vanishes as soon as the Zeeman resonances are further displaced. In fig. 10 the transitions which correspond to the observed lines are reported.

The resonances have been identified by means of a diagram, as that reported in fig. 11, which reproduces the experimental situation: at a fixed frequency ν_1 and for different values of the low frequency ν_2, the calculated position in the magnetic field of the resonances has been represented. The diagram of fig. 11 shows some experimental points for the different lines and the respective

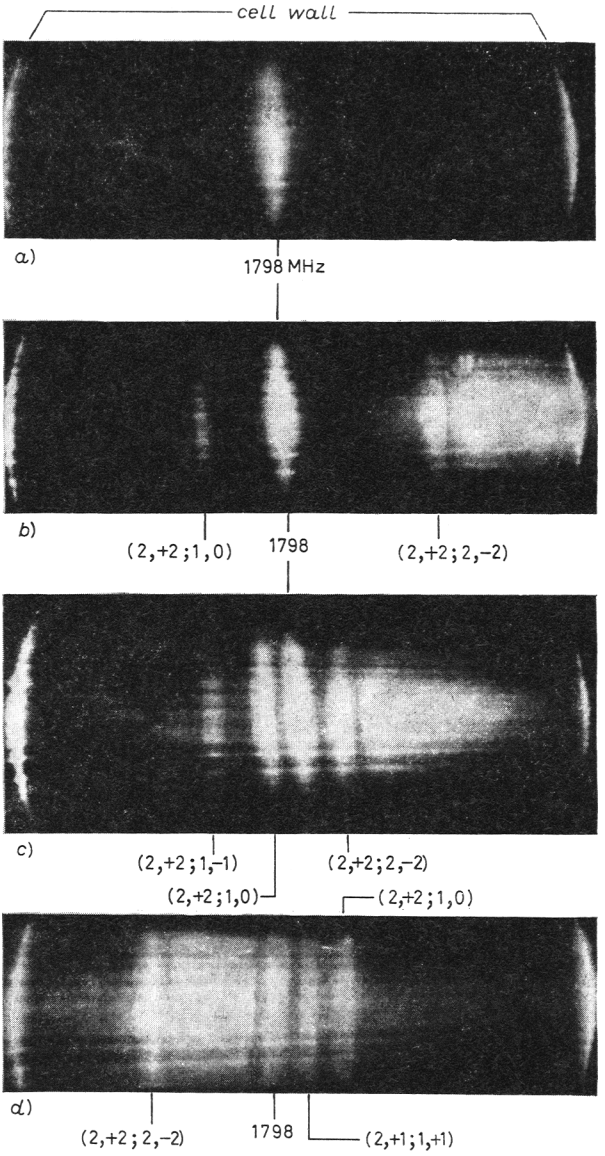

Fig. 9. – **Many-photon transitions between Zeeman hyperfine levels. In all the examples *a*), *b*), *c*), *d*) the frequency ν_1 of the hyperfine field is the same: $\nu_1 = 1798$ MHz, while the frequency ν_2 of the field inducing Zeeman transitions is changed. *a*) $\nu_2 = 9.5$ MHz; *b*) $\nu_2 = 8.9$ MHz (Zeeman pattern visible inside the cell); *c*) $\nu_2 = 8.8$ MHz (Zeeman pattern near to hyperfine transition); *d*) $\nu_2 = 8.5$ MHz (Zeeman pattern on the other side of hyperfine transition).**

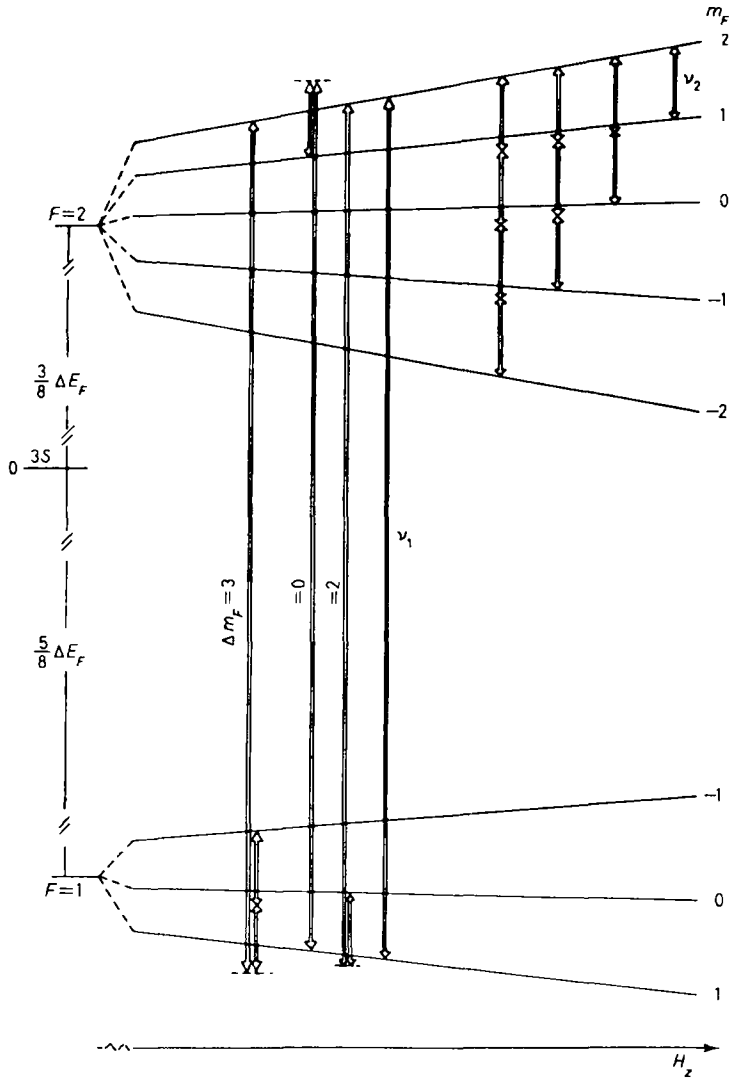

Fig. 10. – Level diagram of the sodium ground state with the observed transitions drawn.

positions determined by the equations

$$H_z = H_z^0$$

for the (2, + 2; 1, + 1) hyperfine line,

$$\nu_2 - \nu_2^0 = \gamma_2(H_z - H_z^0) - (2 + m_F)\gamma' H_z^2 + 3\gamma' H_z^{0^2}, \quad m_F = +1, 0, -1, -2$$

for the Zeeman lines,

$$\nu_2 - \nu_2^0 = -2\gamma_2 H_z + (\gamma_2 + \gamma_1) H_z^0 - 4\gamma' H_z^2 + 6\gamma' H_z^{0^2}$$

for the (2, + 2; 1, 0) two-photon line,

$$\nu_2 - \nu_2^0 = -\frac{2\gamma_2 - \gamma_1}{2} H_z + \frac{\gamma_1}{2} H_z^0 - \frac{3\gamma'}{2} H_z^2 + \frac{9\gamma'}{2} H_z^{0^2}$$

for the (2, + 2; 1, − 1) three-photon line,

$$\nu_2 - \nu_2^0 = -(\gamma_2 + \gamma_1)(H_z - H_z^0) - 6\gamma' H_z^2 + 6\gamma' H_z^{0^2}$$

for the (2, + 1; 1, + 1) two-photon line,

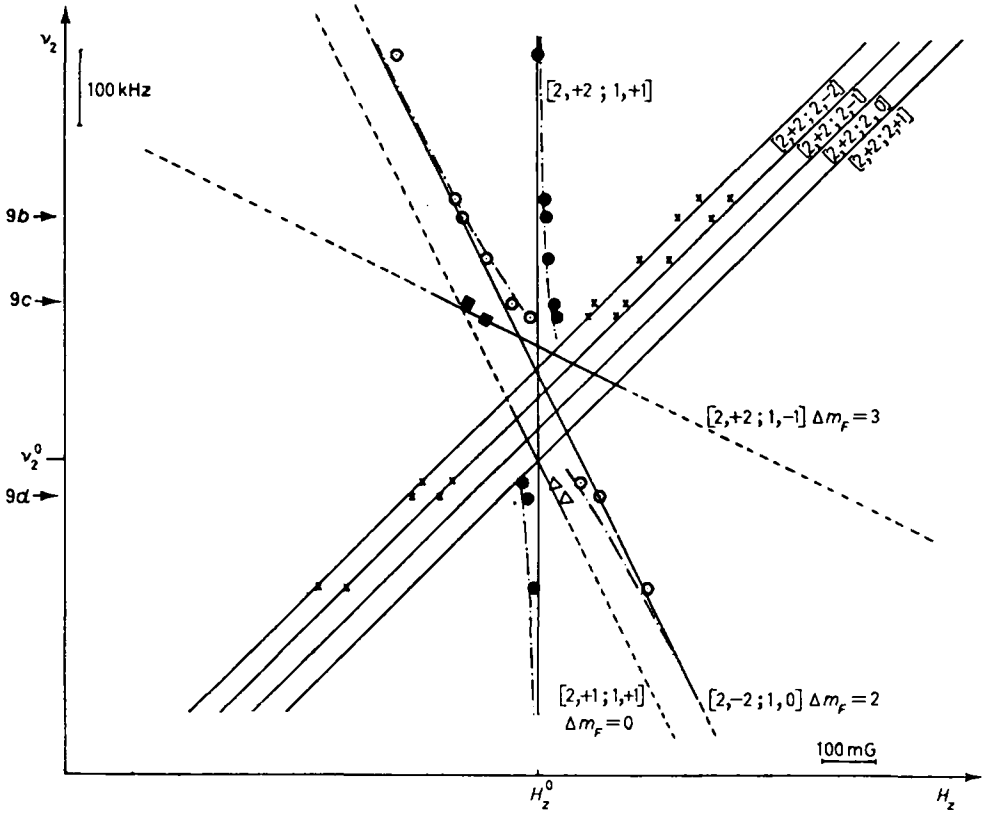

Fig. 11. – Plot of the calculated and observed positions of hyperfine, Zeeman and many-photon transitions. For a given value of ν_2, the positions of the different transitions in the inhomogeneous magnetic field can be obtained by the intercepts of the lines of the plot with a parallel to the H-axis. Arrows indicate the situation of pictures 9*b*), *c*) and *d*). The chain curves represent the shifted positions of the (2, + 2; 1, + 1) and (2, + 2; 1, 0) transitions.

which relate, for each transition, its position H_z to the low frequency ν_2. H_z^0 is the resonance field for the fixed hyperfine transition and ν_2^0 is the resonance frequency of the $(2, +2; 2, +1)$ transition in the H_z^0 field. The regions where the lines show an appreciable intensity are marked with solid lines.

The $(2, +2; 1, 0)$ line is a two-photon transition with an intermediate level, whose intensity is proportional to

$$\frac{\mu_{11,22}^2 H_1^2 \mu_{11,10}^2 H_2^2}{\Delta_{11,10}^2},$$

where $\mu_{Fm_F,F'm_F'}$ is the matrix element of the magnetic-dipole moment and $\Delta_{Fm_F,F'm_F'}$ is the difference between the frequency of the $(F, m_F; F', m_F')$ transition and that of the corresponding applied field. Similarly the three-photon line $(2, +2; 1, -1)$ shows an intensity behaviour proportional to

$$\frac{\mu_{11,22}^2 H_1^2 \mu_{11,10}^2 H_2^2 \mu_{10,1-1}^2 H_2^2}{\Delta_{10,1-1}^2 \Delta_{11,1-1}^2}.$$

These two lines connect the $(2, +2)$ very populated sublevel with a depleted one. Rather unexpected is the third line, $(2, +1; 1, +1)$, which connects, via a two-photon transition, two depleted levels and results to be enough intense only when the power-broadened $(2, +2; 2, +1)$ line occurs very close to the hyperfine line.

The existence of the $(2, +1; 1, +1)$ line has been discussed in a recent paper by DI GIACOMO and FEO [7], where the position, the intensity and the width of the lines have been calculated by taking into account simultaneously the optical pumping and the interaction with the radiofrequency fields. The calculations of ref. [7] are performed under the hypotesis of « broad excitation » and in the absence of buffer gas, but we think that they are, at least qualitatively, valid also for our experimental conditions. In particular, the ratio of the intensities between the $(2, +1; 1, +1)$ and $(2, +2; 1, +1)$ lines follows the factor

$$\frac{\mu_{20,21}^2 H_2^2}{\Delta_{21,22} \Delta_{20,22}},$$

as given by the theory.

The $(2, +2; 1, +1)$ hyperfine line shows a shift with a dispersive behaviour, which is centred at the point where the resonances cross together. This radiative shift is produced by the low-frequency field when, being out of resonance for $(2, +2; 2, +1)$ and $(1, +1; 1, 0)$ transitions, it perturbs

---

[7] A. DI GIACOMO and F. FEO: *Nuovo Cimento*, **30** B, 193 (1975).

the energy of the sublevels and therefore shifts the $(2, +2; 1, +1)$ hyperfine line. Following the notation of ref. ([7]), for the shift we have

$$S_{11,22} = -\left(\frac{\mu_{21,22}^2 H_2^2}{\Delta_{21,22}} + \frac{\mu_{11,10}^2 H_2^2}{\Delta_{11,10}}\right).$$

The shifted position for $H_2 = 100$ mG has been plotted in fig. 11 as calculated by taking into account the line width and in the approximation in which the Δ are calculated for the unperturbed Zeeman levels.

Similar shifts are expected for the other lines. In particular, for the $(2, +2; 1, 0)$ line we have

$$S_{10,22} = \left(-\frac{\mu_{11,22}^2 H_1^2}{\Delta_{11,22}} - \frac{\mu_{21,22}^2 H_2^2}{\Delta_{21,22}} + \frac{\mu_{11,10}^2 H_2^2}{\Delta_{11,10}} - \frac{\mu_{10,1-1}^2 H_2^2}{\Delta_{10,1-1}}\right).$$

In fig. 11 the calculated perturbed position of the $(2, +2; 1, 0)$ line for $H_2 = 100$ mG and $H_1 = 50$ mG has been also reported, but the actual measurements do not show enough accuracy for a comparison with the theory.

5. – « Black lines » by multimode laser light excitation.

In the absence of any r.f. field, the path of the circularly polarized laser beam can be made easily visible inside the cell by slightly turning the axis of the magnetic field as to make a certain angle $\alpha \neq 0$ with the direction of the beam. In this case the pumping process is no longer completely efficient, due to the presence of a π-component of the light in the direction of the magnetic field. Therefore a fluorescence of Na atoms, whose intensity increases with α, appears along the path of the beam. If the method of the magnetic gradient field is used and the laser emission consists of many axial modes, it is possible to observe on the path of the σ^- circularly polarized beam some narrow « black lines » which cross the fluorescence, as can be seen in fig. 12. A first survey of the effect showed the existence of three black lines, whose position along the beam was dependent both on the value of the magnetic field and on the laser mode spacing.

As a matter of fact, in our experimental arrangement the mode pattern of the laser emission consists of many axial modes, which overlap the D_1 line with a frequency interval $\Delta\nu$ of 290 MHz (dye cavity length $L = 51.7$ cm, $\Delta\nu = c/2L$). With this mode spacing the three black lines have been found at 15, 23 and 52 G, respectively. If the cavity length is modified in order to change the mode spacing, the three black lines change their positions in the magnetic field. In any case the most « intense » black line is the first one, *i.e.* that at the lower value of the magnetic field, the other ones being of rather difficult observation.

The existence of black lines can be argued by the work of Bell and Bloom ([8]) on optical pumping in transversal magnetic field. In the Bell and Bloom experiment the magnetic resonance of alkali atoms has been detected by

Fig. 12. – Black lines as observed by tilting the magnetic field to make an angle of $\sim 10°$ with the direction of the pumping radiation. The bright spot, due to the $(2, -2;\ 2, -1)$ r.f. transition, is used for calibrating purposes.

the amplitude modulation of the circularly polarized light without any use of r.f. fields. If the precession of the paramagnetic atoms is synchronous with the frequency of modulation of the light, no absorption of light occurs by the atoms, which are completely oriented and left unperturbed in the transversal magnetic field. On the contrary, if the frequency of the modulation does not match the precession frequency, strong light absorption and fluorescence take place. In our experiment with a multimode laser emission, owing to interference between the modes, we have an amplitude modulation of the light beam at frequencies of the order of the hyperfine transition. As a matter of fact, the interference between one mode and the sixth next one results in an amplitude modulation (beats) at 1740 MHz ($6 \times 290 = 1740$ MHz). This frequency is, therefore, very near to the hyperfine-transition frequency (1771 MHz), as can be seen also from fig. 3, and can be exactly matched to the frequency difference between $(2, -2)$ and $(1, -1)$ levels by a weak magnetic field ($E(2, -2) - E(1, -1) = 1740$ MHz for a field of 15 G). Now the 1740 MHz amplitude modulation frequency also matches the $(2, -1;\ 1, -1)$ and $(2, -1;\ 1, 0)$ transition frequencies at higher magnetic fields.

By changing the light polarization into σ^+, black lines occur at other static-field values, which match the $(2, +2;\ 1, +1)$ and $(2, +1;\ 1, +1)$ transitions to the frequency difference between two other laser modes.

([8]) W. E. Bell and A. L. Bloom: *Phys. Rev. Lett.*, **6**, 280, 623 (1961).

Some measurements of the positions of the black lines in the magnetic field have been performed for different beat frequencies as obtained by displacing the exit mirror of the dye cavity. The mode separation has been calculated by the direct measurement of the cavity length, and the light modulation frequency has been estimated by taking into account the frequency distance between 7 or 6 modes.

The values of the magnetic field at the positions of the black lines have been found by superposing to the black lines the spot of fluorescence of the $(2, -2; 2, -1)$ transition as obtained by a tunable r.f. field and by applying the Breit-Rabi formula to the measured frequencies.

The results have been compared in the plot shown in fig. 13. The curves give, in MHz, the calculated values of the distance between the sublevels of

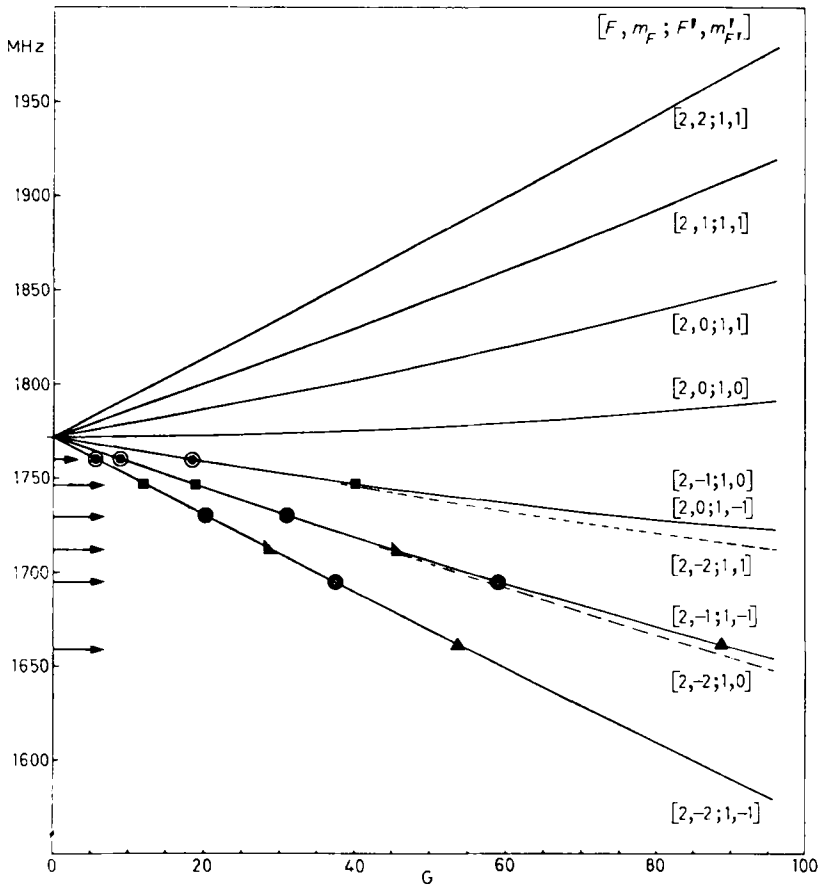

Fig. 13. – Position of the observed black lines in the magnetic field. The beat frequencies, as calculated by the measurement of the dye cavity length, have been indicated by arrows. Experimental points are compared with the calculated hyperfine-transition frequencies in the same field.

the hyperfine structure *vs.* the magnetic field. If we trace for a given value of the beat frequency a parallel to the x-axis, the intercepts with the lines of the drawing give the position in the magnetic field of the black lines. Arrows indicate for six different beat frequencies the experimentally found positions of the black lines.

Other experiments on the modalities of this phenomenon are in progress. On the other hand, while this manuscript was submitted to publication, a theoretical analysis taking into account coherence phenomena in a three-level system has been performed (9), which can be related to the observed effect.

(9) E. ARIMONDO and G. ORRIOLS: *Lett. Nuovo Cimento*, **17**, 333 (1976).

● RIASSUNTO

Si presenta un nuovo metodo che permette l'esame diretto di transizioni a più fotoni, di allargamento di righe e di spostamento di risonanze prodotto da intensa radiazione laser in vapori di sodio orientati otticamente. Con questo metodo si è messo in evidenza un fenomeno dovuto a battimenti tra modi di un laser a coloranti usato per il pompaggio ottico.

Экспериментальный метод наблюдения радиочастотных переходов и резонансы лазерных биений в ориентированных парах натрия.

Резюме (*). — Предлагается новый метод, который позволяет непосредственно исследовать многофотонные переходы, уширение линий и смещение резонанса, образованного интенсивным излучением лазера в оптически ориентированных парах натрия. С помощью этого метода подтверждается явление биений мод лазера в красителях, используемых для оптической накачки.

(*) *Переведено редакцией.*